

Development of the Deployable HF Vector Sensor for the AERO-VISTA Spacecraft

Mark Silver
MIT Lincoln Laboratory
244 Wood St
Lexington, MA 02421
mark.silver@ll.mit.edu

Erik Thompson
MIT Lincoln Laboratory
244 Wood St
Lexington, MA 02421
erik.thompson@ll.mit.edu

Mary Knapp
MIT Haystack Observatory
99 Millstone Road
Westford, MA 01886
mknapp@mit.edu

Lenny Paritsky
MIT Haystack Observatory
99 Millstone Road
Westford, MA 01886
lparit@mit.edu

Kristen Ammons
MIT Department of Aeronautics and Astronautics
77 Massachusetts Avenue
Cambridge, Massachusetts 02139
kjammons@mit.edu

Ekaterina Kononov
MIT Department of Aeronautics and Astronautics
77 Massachusetts Avenue
Cambridge, Massachusetts 02139
kkon@mit.edu

Alai Lopez
MIT Lincoln Laboratory
244 Wood St
Lexington, MA 02421
alai.lopez@ll.mit.edu

Alexander Morris
MIT Lincoln Laboratory
244 Wood St
Lexington, MA 02421
alexander.morris@ll.mit.edu

Philip Erickson
MIT Haystack Observatory
99 Millstone Road
Westford, MA 01886
pje@mit.edu

Rebecca Masterson
MIT Kavli Institute for Astrophysics and Space Research
77 Massachusetts Avenue
Cambridge, Massachusetts 02139
becki@mit.edu

Nicholas Belsten
MIT Department of Aeronautics and Astronautics
77 Massachusetts Avenue
Cambridge, Massachusetts 02139
nbelsten@mit.edu

Cadence Payne
MIT Department of Aeronautics and Astronautics
77 Massachusetts Avenue
Cambridge, Massachusetts 02139
cbpayne@mit.edu

Daniel Howe
MIT Lincoln Laboratory
244 Wood St
Lexington, MA 02421
daniel.howe@ll.mit.edu

Alan Fenn
MIT Lincoln Laboratory
244 Wood St
Lexington, MA 02421
ajf@ll.mit.edu

Frank Lind
MIT Haystack Observatory
99 Millstone Road
Westford, MA 01886
flind@mit.edu

Abstract—The Auroral Emissions Radio Observer (AERO) and Vector Interferometry Space Technology using AERO (VISTA) CubeSat missions will use two identical 6U CubeSats developed to measure HF auroral emissions from Low Earth Orbit for NASA’s Space Mission Directorate (SMD) for Heliophysics. Each CubeSat employs a unique antenna, called a Vector Sensor Antenna (VSA), to measure all six electromagnetic degrees of freedom of incoming HF radiation via a combination of loop, dipole and monopole antennas. The VSA payload stows into a compact volume within the 6U spacecraft, and through a series of deployments, makes a 4 m by 4 m by 2.3 m antenna array. The relatively large antenna element deployment from such a small initial volume is achieved using fiberglass composite tape springs which unroll to form the antenna elements. These tape springs fall into a class of structural elements called High Strain Composites, which are becoming more commonly used in space missions. This paper describes the development, integration and testing of the AERO-VISTA VSA payload prototype.

DISTRIBUTION STATEMENT A. Approved for public release. Distribution is unlimited. This material is based upon work supported by the Department of the Air Force under Air Force Contract No. FA8702-15-D-0001. Any opinions, findings, conclusions or recommendations expressed in this material are those of the author(s) and do not necessarily reflect the views of the Department of the Air Force.
©2023 Massachusetts Institute of Technology. Delivered to the U.S. Government with Unlimited Rights, as defined in DFARS Part 252.227-7013 or 7014 (Feb 2014). Notwithstanding any copyright notice, U.S. Government rights in this work are defined by DFARS 252.227-7013 or DFARS 252.227-7014 as detailed above. Use of this work other than as specifically authorized by the U.S. Government may violate any copyrights that exist in this work.

TABLE OF CONTENTS

| | |
|---|---|
| 1. INTRODUCTION..... | 1 |
| 2. SPACECRAFT OVERVIEW..... | 2 |
| 3. VECTOR SENSOR ANTENNA..... | 2 |
| 4. VSA MECHANICAL DESIGN MODIFICATIONS AND RISK REDUCTION | 3 |
| 5. VSA RF MEASUREMENTS | 7 |
| 6. CURRENT STATUS | 7 |
| 7. CONCLUSIONS..... | 7 |
| ACKNOWLEDGMENTS | 7 |
| REFERENCES | 8 |
| BIOGRAPHY | 8 |

1. INTRODUCTION

AERO and VISTA are identical, 6U, spacecraft being developed by MIT Haystack Observatory, the MIT AeroAstro department and MIT Lincoln Laboratory. The goal of the AERO CubeSat mission is to investigate the nature and sources of auroral HF (100 kHz-15 MHz) emissions [1]. HF emissions from aurora typically do not reach the ground due to Earth’s ionosphere, therefore these measurements can only be done from space [2]. The specific primary goals for AERO & VISTA are to:

1. Validate the use of electromagnetic vector sensors for localization of Auroral radio sources,
2. Investigate the generation and propagation of radio emissions such as Auroral Kilometric Radiation (AKR),
3. Explore the electromagnetic wave environment of the Earth below the ionospheric cutoff, and
4. Demonstrate dramatically improved angular resolution using interferometry in space with both controlled ground beacons and Auroral emissions.

The common AERO and VISTA spacecraft is called AERO-VISTA. Each spacecraft contains a deployable Vector Sensor Antenna (VSA), shown deployed in Figure 1, that is comprised of loops, dipoles and a monopole, which make up the main sensor for the mission. The two spacecraft will be launched together and released at the same time into a local noon sun-synchronous, 450-600 km altitude, polar orbit. They will use differential drag to slowly separate during their 90-day mission. The VSA on both AERO and VISTA can individually fully characterize incoming HF radiation, but measurements from the two spacecraft will be combined interferometrically to better geolocate HF sources.

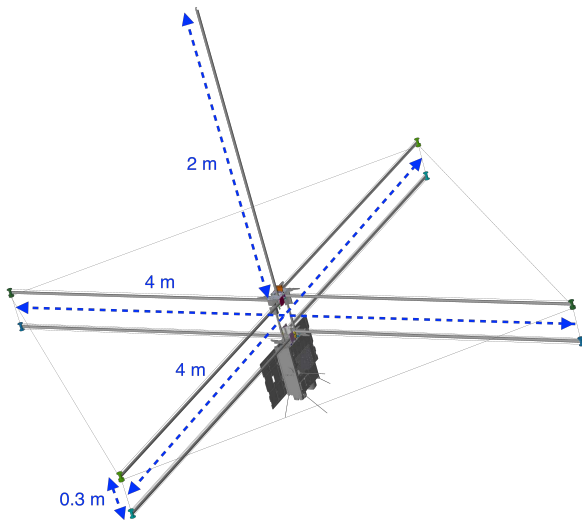


Figure 1. The AERO-VISTA spacecraft CAD model shown in its final deployed state with major dimensions.

This paper will present the design of the deployable antenna, the integration and testing of engineering model antenna into the non-flight spacecraft, and the results of further design updates and mechanical risk reduction tests.

2. SPACECRAFT OVERVIEW

The AERO-VISTA spacecraft consists of a custom 6U satellite bus, developed by NanoAvionics, and the mission payloads, consisting of the Aurora Radio and two identical Auxiliary Sensor Payloads (ASP) and the VSA. The spacecraft and the associated payload packaging are shown in Figure 2. The spacecraft provides all communications, commanding, attitude determination and control, and power generation, storage and distribution. The Aurora Radio serves as the mission radio and payload controller, providing the communication and power link between the payloads and the bus. Details about the Aurora Radio can be found in [3].

The ASP was designed and built by students at MIT. The two identical ASP units in each spacecraft will capture magnetic

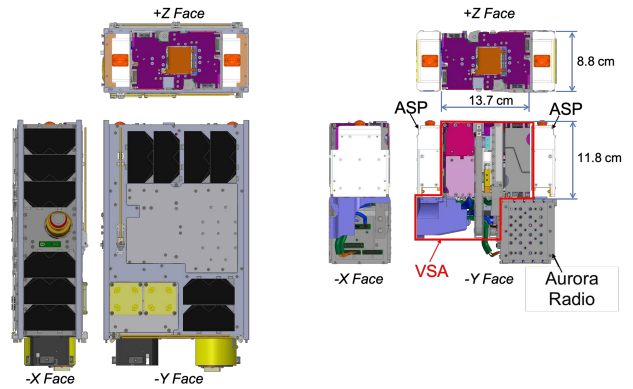


Figure 2. Packaging of the VSA, Electronic Payload and ASP units, with spacecraft bus frame (left) and without spacecraft bus frame (right).

and optical data simultaneously with the VSA to contextualize the measured auroral radio emissions [4, 5]. Additionally, the ASP has an engineering optical fish-eye camera to verify deployment of the VSA and to provide contextual imagery during science operations [6].

The VSA and Aurora Radio were designed and built by MIT LL and are provided to MIT Haystack Observatory for spacecraft integration. The VSA is the main science instrument for AERO-VISTA and is the main focus of this paper. It is described in more detail in the following section.

3. VECTOR SENSOR ANTENNA

The VSA is a collection of loop, dipole and monopole antennas that together can fully characterize incoming HF emissions [2, 7]. These antenna elements are highlighted in Figure 3. The VSA and Aurora Radio are able to measure emissions between 100 kHz-15 MHz, but is optimized for the science mission to measure between 400 kHz-5 MHz [8].

While the antenna is small relative to the wavelengths it is measuring, as Figure 2 shows it is very large compared to the spacecraft. Therefore the antenna must be packaged for launch and deployed once on orbit. This is achieved through the use of high-strain composite tape measure members, which unfurl when released to form the structural backbone of the VSA and also carry the wire used to make the antenna elements [9]. These unique deployable elements allow the 4-meter by 2-meter antenna to stow for launch in a 1.4 L volume. The mass of the VSA and its associated deployment mechanisms and cables is 1.7 kg.

After the spacecraft reaches orbit, is stabilized and has deployed its solar panels, the spacecraft will be commanded from the ground to initiate the VSA deployment. The deployment is achieved over three steps. These three steps are shown in Figure 4, and details of the mechanisms used to enable each deployment step have been described previously [9]. First, the stowed VSA must be extended out of the spacecraft to become clear of the structural panels. Second, the top half of the VSA is extended up to create the height needed for the vertical loops. As this extension happens, the composite booms that carry the loop/dipole wires are released to freely unroll. Finally, the monopole is deployed by releasing a composite boom with the monopole wire to freely unroll. Each of these steps is initiated through separate release mechanisms

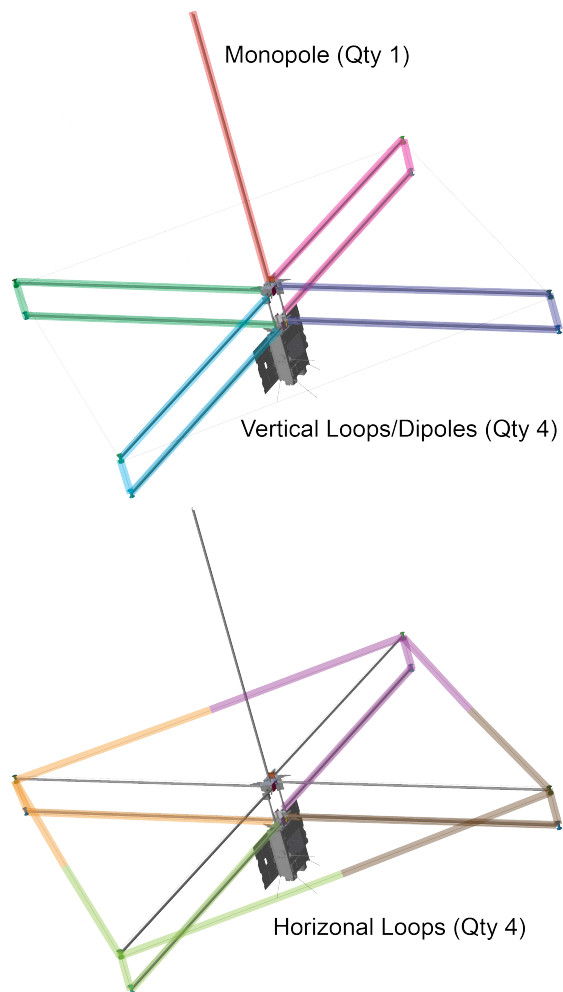


Figure 3. The antenna elements that make up the VSA, each highlighted in different colors.

and each release mechanism is commanded independently, so that the deployment process can be phased as needed to accommodate monitoring of the success of each deployment step.

To date, a non-flight prototype of the VSA has been built and tested. This prototype was called the Delta Model (DM) version of the VSA. The purpose of making the DM was to validate the concept and perform mechanical and RF testing to identify modifications needed for the Flight Model (FM). The next section describes the design modifications identified as a result of the DM VSA deployment testing and further risk reduction activities completed after the testing.

4. VSA MECHANICAL DESIGN MODIFICATIONS AND RISK REDUCTION

The DM VSA was designed, assembled and tested at the payload-level at MIT LL. Although this unit was not designated a flight unit, it received the same rigor in material selection and cleanliness required for a Flight Model (FM). During the initial assembly of the DM VSA, several risk reduction tests were completed to ensure that each separate deployment mechanism worked independently and to show that the higher risk deployment actuators had sufficient force margin. These

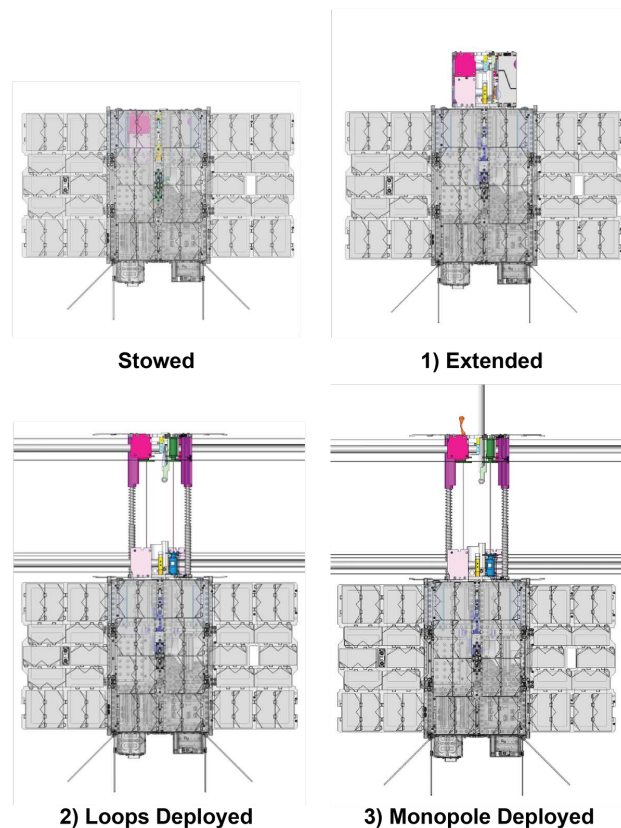


Figure 4. The stowed VSA and the three steps of the VSA deployment sequence.

initial tests were mostly successful and highlighted several remaining risks. A detailed description of these tests was previously published [9]. The following mechanical design-related risks were identified that could result in deployment failure:

1. The extension deployment mechanism wears easily and is very sensitive to misalignment.
2. The release mechanisms for each deployment step have insufficient force margin for the extension and loop deployment.
3. The 3D-printed plastic housing that contains the compression springs that drive the loop deployment break easily.
4. Friction in the monopole housing makes the deployment unreliable.

In addition to these design-related risks, there were key risks for the VSA that had not been reduced in this DM testing which could result in deployment failure, namely:

5. The VSA mechanical components may fail under launch vibration loads.
6. The as-built VSA may not have the RF sensitivity predicted by modeling.
7. Cold or hot extreme temperatures could cause malfunction in deployment mechanisms.

Design modifications were developed to address risks 1-4 and testing was performed to address risks 5 and 6. These

are described in the next section. The AERO-VISTA team has determined that risk 7 can be retired by limiting the deployment to times when the VSA is within a predetermined temperature range, which will be possible due to the local noon sun-synchronous polar orbit.

Extension Deployment Mechanism Design Modifications

The first risk required the most significant design modification. To reduce this risk, an alternate approach was used to allow the extension motion. Initially, the extension motion was enabled through parallel shafts and cylindrical bearings, as described in [9]. The modified design uses standard 5mm linear guide rails and carriages, and is shown in Figure 5. The linear guide rail approach was considered because the carriages have more compliance than a cylindrical bearing, which should result in less sensitivity to misalignment.

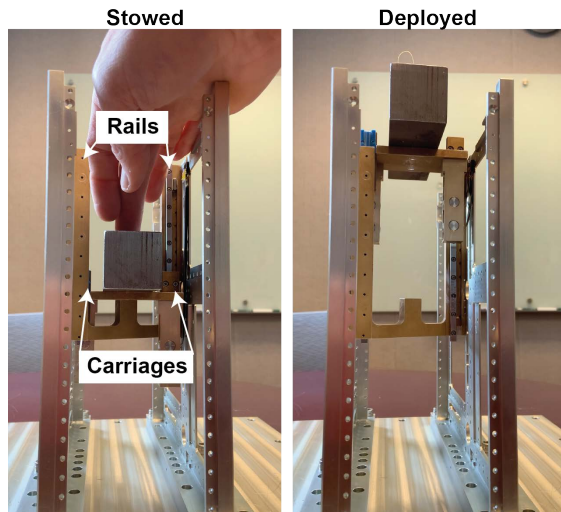


Figure 5. Prototype of linear guide rail and carriage extension slider stowed (left) and deployed (right).

These standard carriage and rail systems have well documented limit loads. A worst-case loading analysis, which assumed that a malfunction occurred such that a single carriage experienced all of the possible moment loads, showed that the carriages have sufficient margin. Based on this analysis, an experimental prototype was built to investigate the design and validate the ability to accommodate misalignment due to enforced expansion or compression at the top of the extension stage. The test apparatus and extension mechanism prototype are shown in Figure 6.

In these tests, the top edges of the opposites sides of the Test Frame were either compressed together or spread apart. Figure 6 shows the configuration where they are spread apart by two spreaders. For the compression tests, the top edges of the opposite sides of the Test Frame were pushed together with a large c-clamp. The deflection indicators on either side measure the amount of expansion or compression. During the tests, the amount of expansion or compression was slowly increased between tests and the VSA mass simulator was deployed. The deflection indicator measurements were recorded and any change in the rate of deployment was noted. The compression or expansion was increased until the extension deployment would not fully extend.

The test results are shown in Table 1. These results show that the prototype rail and carriage deployment mechanism can operate with no noticeable change in deployment rate with

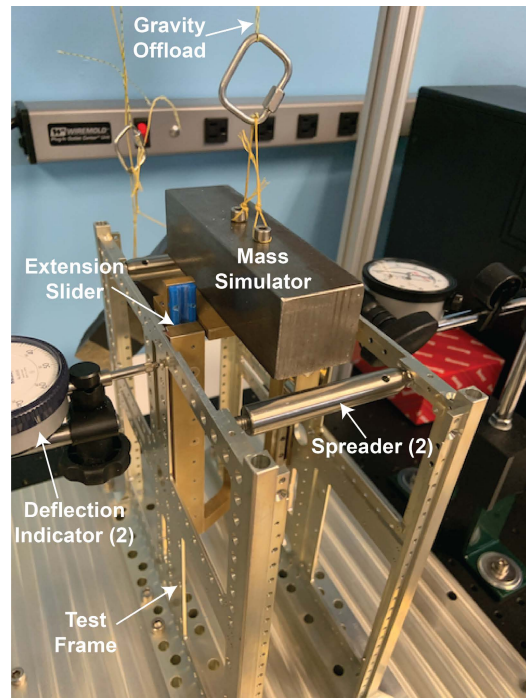


Figure 6. Linear guide rail and carriage extension mechanism prototype testing to validate performance under misalignment.

up to 0.50 mm of compression and 0.30 mm of expansion at the top of the mechanism. Nominally, the dimension between the two interfacing sides of the spacecraft where the VSA mounts is 95.00 mm. Measurements along this interface from the Engineering Development Unit (EDU) spacecraft found that as-built dimensions were 95.09-95.14 mm. This indicates an expansion of up to 0.14 mm, which is well within the 0.30 mm that the rail and carriage extension mechanism can accommodate with no noticeable change in deployment speed.

Table 1. Test results for rail and carriage expansion mechanism misalignment limits.

| Condition | Compression (mm) | Expansion (mm) |
|-----------|------------------|----------------|
| No Change | 0.50 | 0.30 |
| Slowed | 0.72 | 0.48 |
| Stopped | 0.73 | 0.57 |

Based on these results, the extension mechanism design is being updated to adopt the rail and carriage design. There are still some aspects of the design that require further development, including determining the proper lubricant for the carriages that will work in the space environment. There are several options that can be used or the carriages could be used without lubricant. The proper lubricant will be determined in future experiments.

Release Mechanism Force Margin

The release mechanism used for each stage of deployment is the nD3PP shape-memory alloy pin-puller developed by DeployablesCubed GmbH. This mechanism was fairly new at

the beginning of the AERO-VISTA programs, but it offered many benefits when compared other options. The key benefits of using this release mechanism for AERO-VISTA are that it is compact and very easy to reset. More about this pin-puller mechanism and their use in AERO-VISTA can be found in [9].

While initial testing showed that the pin-pullers should have sufficient force margin to retract for all deployments, the amount of preload on the pin was difficult to repeatably control each time the VSA was stowed. Therefore, the decision was made to consider redesigning the higher preloaded deployments, the extension and loop deployments, with a release nut from the same manufacturer. The nD3RN reacts the load axially through the nut, while the nD3PP reacts the load in shear and bending along the pin. Based on this loading difference, the nD3RN can operate under up to five times the preload of the pin-puller, but has the same small form-factor and is just as easy to reset. Incorporating the release nut required rotating the actuation direction in the design. This change has been accommodated in the design without issues. Future testing of a non-flight version of the release nut will verify performance under the higher preload.

Compression Spring Housing

Several parts within AERO-VISTA were designed to be 3D printed using FDM of ABS plastic due to their complexity. One particular 3D printed part is used to contain the compression spring that drives the telescoping action during the loop deployment step. Details about the mechanisms used for this deployment can be found here [9]. While the housing worked to contain the compression spring, the process of stowing the spring repeatedly weakened the thin walls of the 3D printed part and results in repeated failures. Therefore, the housing was redesigned in aluminum and to be manufactured through traditional machining. This new design is much more resilient than the ABS version. However, the compression spring experiences more friction from the inside of the aluminum version, which can keep the loop deployment from initiating. Further development is underway to reduce or overcome this friction through better control of the surface roughness or by adding a kick-off spring to initiate the loop deployment.

Monopole Release

The monopole deployment is enabled by releasing a coiled tape measure-like boom which carries the monopole antenna wire. Figure 7 shows a diagram of the stowed monopole in a model cross-section. In working with the DM VSA, it was found that after some amount of handling of the VSA with the monopole stowed, it would not unfurl from the stowed volume when the monopole door was opened. This is likely due to the fact that the strain in the coiled boom forces the coil to expand as it is jostled through release of static friction in the coil. At some point it expands so much that it is preloaded against the side of the monopole constraint box and does not unfurl due to friction.

The proposed solution to this problem is to add a kick-off spring underneath the coiled boom such that as the monopole door is released, the coil is pushed clear of the monopole constraint box so that it can start to unfurl. A concept for the kick-off assembly is shown in Figure 8. This design will be prototyped and tested before final implementation into the final FM design.

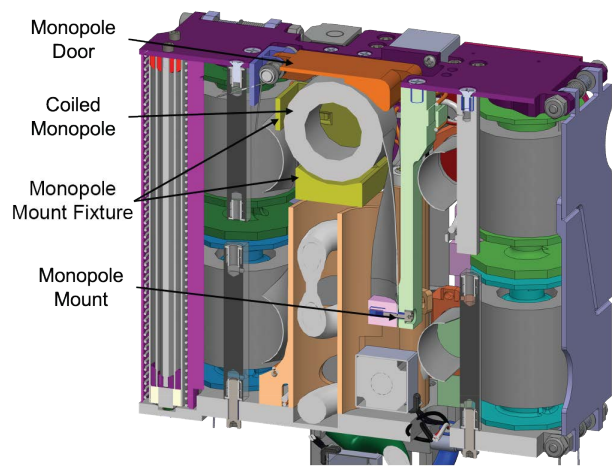


Figure 7. Diagram of the DM model cross-section showing the stowed monopole.

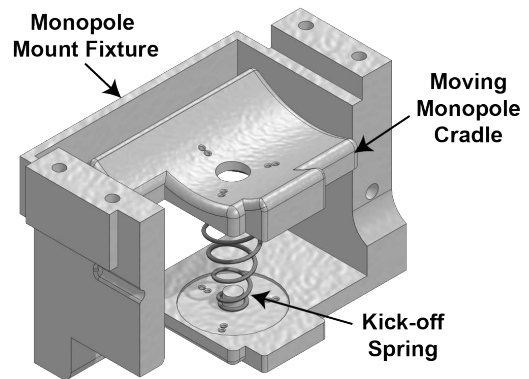


Figure 8. Concept for monopole kickoff spring.

VSA Vibration Testing

For a typical space flight program, a finite element model is used to simulate the response to random vibration, which simulates the launch environment, and estimate the stresses in the components to determine stress margins. The scope and risk posture for the AERO-VISTA missions offered only minimal mechanical finite element analysis of the VSA. Therefore, the risk of failure during launch was to be reduced through random vibration testing. This testing only was performed with the DM VSA after all other testing and RF measurements of the VSA was complete in case of a failure during testing.

In order to replicate the true boundary conditions for launch, the VSA ideally would be installed in the spacecraft. However, the EDU spacecraft was still needed for other parts of the project and could not risk potential damage if the VSA failed during testing. Therefore, a stand-in structure was designed and built for the vibration tests. This stand-in also had components inside it that simulated the mass and inertia of the actual spacecraft components. There was no attempt to match the stiffness of the actual spacecraft components. A photograph of the DM VSA installed in the stand-in spacecraft in its post-vibration deployment testing configuration is shown in Figure 9.

For vibration testing, CubeSats are typically installed in a frame that mimics the deployer box that they are held in

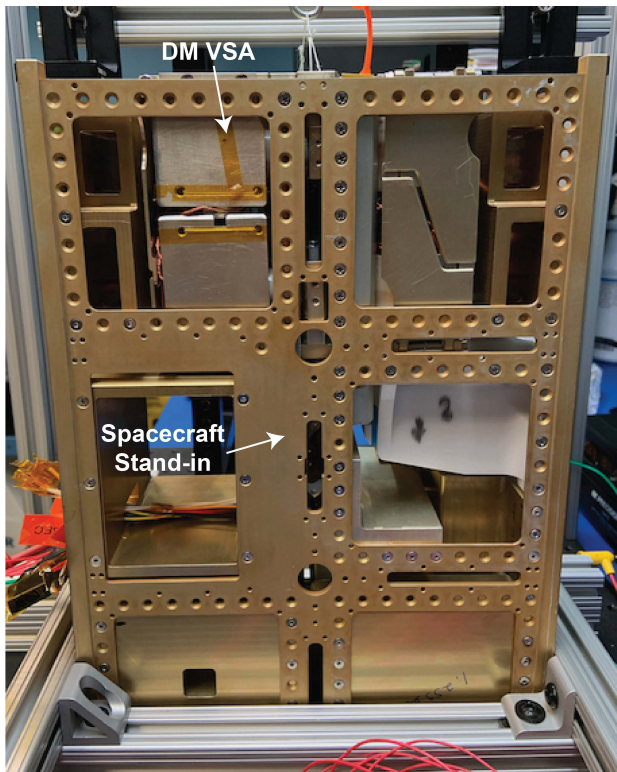


Figure 9. Photograph of DM VSA within the spacecraft stand-in installed in the post-vibration deployment test frame.

during launch. This test frame is called a test-pod. A test-pod available from a previous 6U CubeSat program was available and was used for these tests. The DM VSA and the stand-in spacecraft are shown inside the vibration test-pod in Figure 10. This figure all shows the test coordinate axes and the locations of accelerometers used to monitor the test.

Because the specific launch vehicle that will be used for the AERO-VISTA launch is unknown, the vibration testing performed using random vibration spectrum defined in NASA's GEVS [10]. The initial plan was to start with acceptance level vibration, then move up to proto-qualification level, then to qualification level, with deployment tests occurring after testing in each axis (X, Y and Z) at each level. Vibration testing would only advance through the test plan if the DM VSA survived and successfully deployed. However, due to Ground Support Equipment (GSE) related issues and availability of the vibration tables, the test campaign needed to be compressed. This resulted in skipping the first set of deployment tests planned after Y-axis Acceptance-level vibration and later skipping the Proto-Qualification-level tests all together and moving right from Acceptance-level to Qualification-level.

Vibration testing was performed on one of MIT LL's two Unholtz-Dickie T2000 shaker systems with an integrated slip table. The Y- and X-axes were tested using the slip table, while the Z-axis used the vertical orientation. Therefore, Y- and X-axes were tested before the Z-axis. X-axis testing was considered higher risk because it loads all three of the pin-pullers directly. Therefore, the Y-axis test was performed before the X-axis for each vibration level. Table 2 shows a summary of the post-vibration deployment testing that was performed.

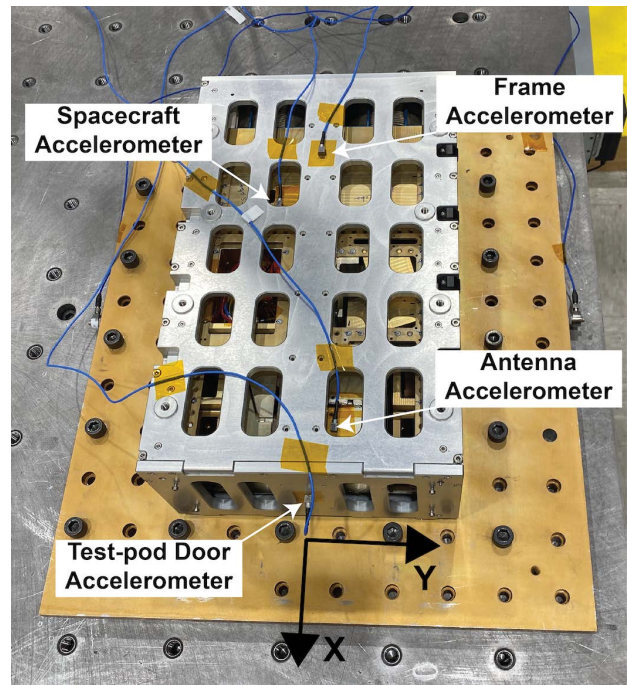


Figure 10. Photograph of DM VSA and spacecraft stand-in installed in the vibration test-pod. The locations of accelerometers are labeled and the test coordinates are shown.

As mentioned previously, because no damage was visible after Y-axis Acceptance-level test, no deployment tests were made after Y-axis Acceptance to expedite testing. Deployment tests after Y and X-Axis Acceptance testing identified an issue with the extension pin-puller. It would not release when commanded. Due to this issue, the telescoping deployment could not be tested because it requires the VSA to be extended out of the spacecraft to deploy. The monopole, however, could be released without the extension deployment and that release was successful.

At this point, the team decided it was best to move on to Z-Axis Acceptance testing to ensure that the VSA could survive vibration in that axis. Deployment tests after Z-Axis Acceptance testing encountered the same pin-puller issue during the extension deployment. After several electrical checks, the team decided that the problem may be a mechanical problem with the pin-puller. Through some experimentation the team found that jostling the pin-puller through its rear reset hole allowed the pin-puller to release when actuated. After discussions with DeployablesCubed, it was determined that the likely cause of this issue was foreign objects or debris (FOD) in the pin-puller housing. The FOD could have been introduced through handling in a non-clean room environment or from excessive cycling of the pin-puller. This problem with the extension pin-puller persisted through the rest of the testing, but the intervention described earlier allowed the pin to retract and deployments were successful.

A second issue was found during the telescoping deployment tests after vibration. The pin-puller would release but the deployment would not initiate. It was found that tapping on the VSA would cause the deployment to initiate and the deployment would successfully deploy. This indicates the presence of too much friction in the interfaces in the stowed configuration. There are several potential sources of friction

Table 2. Post-vibration deployment testing results summary.

| Level | Axis | Extension | Telescoping | Monopole |
|---------------|------|----------------------|-----------------------|------------|
| Acceptance | Y | Not Tested | Not Tested | Not Tested |
| | X | No success | N/A (Needs extension) | Success |
| | Z | Success ¹ | Success ² | Not tested |
| Qualification | Y | Success ¹ | Success ² | Not tested |
| | X | Success ¹ | Success ² | Not tested |

¹ Pin-puller intervention required, ² Assisted initiation of deployment

in this stowed configuration and it is difficult to determine which interfaces are driving this friction. This issue was never identified in the pre-vibration testing, it only occurs after vibration. One likely cause of this increased friction is the compression springs and their aluminum housing.

5. VSA RF MEASUREMENTS

Before vibration and deployment testing, the DM VSA RF performance was tested in the Large Near Field Chamber at the RF Systems Test Facility (RFSTF) at Hanscom Air Force Base, Massachusetts [11]. The purpose of this testing was to demonstrate the ability of the AERO-VISTA VSA and electronics to receive external test signals on all 6 antenna channels at various frequencies and electromagnetic field orientations.

The chamber provided a relatively quiet environment, reducing the strength of potentially interfering signals. All testing was done in the near field, and electromagnetic simulations indicated that effects due to proximity to the walls, ceiling, and floor are negligible as long as the distance between the antenna-under-test and the probe is small compared to the distance to any other conductive object.

The antenna wires were deployed to their full extent and supported using a gravity offload structure consisting of a wooden platform and PVC tubing, as shown in Figure 11. A signal tone was radiated in the near-field of the antenna using an arbitrary waveform generator and a small test probe with controlled position and orientation. The signal received by the Aurora Radio through the VSA was captured and saved to disk. The testing used various frequencies and probe positions. These data were then analyzed and compared to simulated data. A diagram of the simulation model, highlighting Dipole A mode, is shown in Figure 12.

The results for the Dipole B mode are shown in Figure 13. These results show excellent agreement with simulation. The measured amplitudes of the discrete frequency tones that were radiated in the near-field of the dipole were found to track very closely with the expected frequency response of the antenna and receiver electronics. While the Dipole B mode showed good results, the testing procedure revealed issues in some of the other antenna modes. In some cases little to no signal was received, suggesting a simple wiring error or receiver issue. This result is not unexpected given the fact that this is the first testing performed on the system at this level of integration. After the RF testing, continuity checks of the DM VSA alone showed that the antenna wiring was correct. The root cause of these issues will be investigated in future testing.

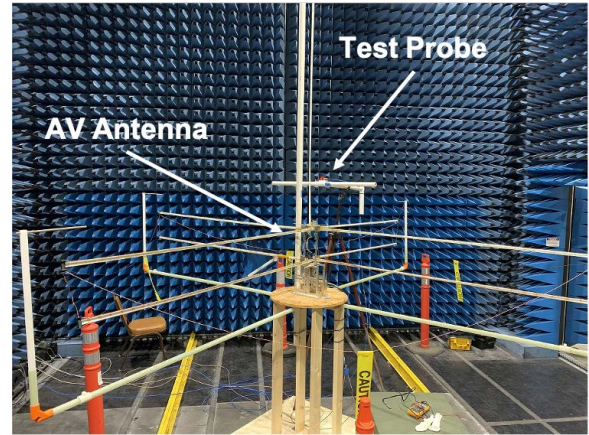


Figure 11. Photo of DM VSA deployed in a test frame in anechoic chamber.

6. CURRENT STATUS

The AERO-VISTA space flight program was put on hold in October 2022 due to the end of the original NASA programs. At this point, the flight spacecraft buses, ASPs and Aurora Radios have been delivered and are being stored in a clean room at MIT Haystack Observatory. During this pause in work, MIT LL internal funds were obtained to pursue the risk reductions described in this paper. The team is working to find further funding opportunities through NASA to bring this program to flight.

7. CONCLUSIONS

This paper presented the results of a variety of risk reduction design and testing tasks for the AERO-VISTA satellite Vector Sensor Antenna payload. The risk reduction work described here addressed key risks which were identified during the development of a non-flight version of the VSA, namely susceptibility to damage during launch vibration, as-built antenna performance, and several deployment reliability related issues. These were all addressed to some extent in the current work, but there is more work needed to fully reduce these risks for the flight model.

ACKNOWLEDGMENTS

The authors thank the MIT LL Advanced Development Committee for their financial support for this work. We would also like to thank Dan Stromberg at MIT LL who provided guidance planning for and executing the vibration testing.

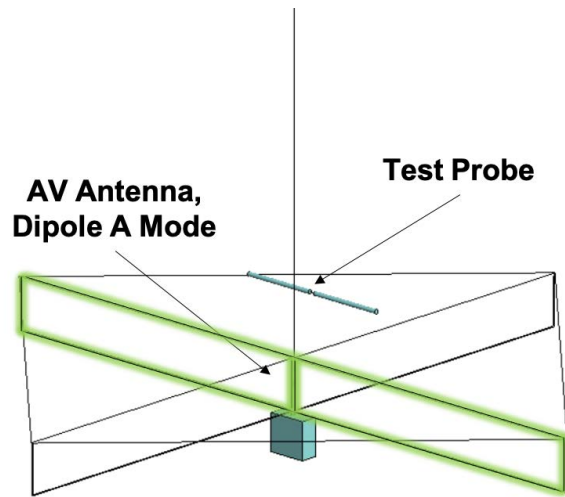


Figure 12. Electromagnetic simulation model of antenna test apparatus.

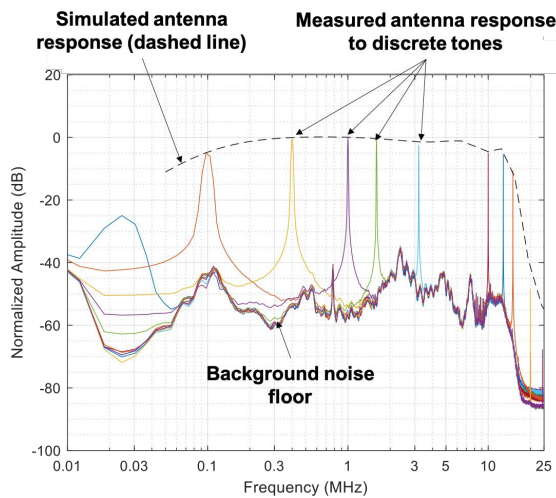


Figure 13. Measured vs. simulated frequency response of the AV antenna Dipole B mode.

REFERENCES

- [1] F. D. Lind, P. J. Erickson, M. Hecht, M. Knapp, G. Crew, R. Volz, J. Swoboda, F. Robey, M. Silver, A. J. Fenn *et al.*, “AERO & VISTA: Demonstrating hf radio interferometry with vector sensors,” in *Small Satellite Conference*. USU/AIAA, 2019.
- [2] M. Knapp, F. Robey, R. Volz, F. Lind, A. Fenn, A. Morris, M. Silver, S. Klein, and S. Seager, “Vector antenna and maximum likelihood imaging for radio astronomy,” in *2016 IEEE Aerospace Conference*. IEEE, 2016, pp. 1–17.
- [3] F. Lind, M. Knapp, P. Erickson, R. McWhirter, R. Schaefer, T. Gedenk, F. Robey, E. Thompson, M. Silver, A. Fenn *et al.*, “Aurora: A software radio for electromagnetic vector sensors in space,” in *Small Satellite Conference*. USU/AIAA, 2022.
- [4] N. Belsten, C. Payne, R. Masterson, K. Cahoy, M. Knapp, T. D. Gedenk, F. D. Lind, and P. J. Erickson, “Design and performance of the AERO-VISTA magnetometer,” in *Small Satellite Conference*. USU/AIAA,

2022.

- [5] C. C. B. Payne, “Auroral arc detection using a COTS spectral photometer for the auroral emission radio explorer (aero) cubesat mission,” Master’s thesis, Massachusetts Institute of Technology, 2020.
- [6] K. J. Ammons, “Concept of operations and failure analysis for a complex deployable cubesat antenna payload,” Master’s thesis, Massachusetts Institute of Technology, 2022.
- [7] F. C. Robey, M. Knapp, A. J. Fenn, M. Silver, K. Johnson, F. J. Lind, R. Volz, S. Seager, and F. Neylon-Azad, “High frequency radio astronomy from a small satellite,” in *Small Satellite Conference*. USU/AIAA, 2016.
- [8] P. J. Erickson, F. D. Lind, M. Knapp, R. Volz, J. Swoboda, A. T. Weatherwax, J. W. LaBelle, F. Robey, A. J. Fenn, B. Perry *et al.*, “LF/HF interferometry in low earth orbit using electromagnetic vector sensors: The AERO-VISTA mission,” in *2023 United States National Committee of URSI National Radio Science Meeting (USNC-URSI NRSM)*. IEEE, 2023, pp. 187–188.
- [9] M. J. Silver, A. Lopez, R. Reeve, A. Morris, and A. Fenn, “Development of the high strain composite deployable vector sensor payload for the AERO and VISTA cubesat missions,” in *AIAA SciTech Forum*, 2023.
- [10] G. E. V. Standard, “NASA publication GSFC-STD-7000,” *General Environmental Verification Standard*, NASA, Goddard Space Flight Center, Maryland, 2005.
- [11] A. Fenn, “The MIT Lincoln Laboratory RF systems test facility for rapid prototyping,” *Microwave Journal*, March 7, 2021.

BIOGRAPHY



Mark Silver received his B.S. degrees in engineering mechanics from the University of Wisconsin, and his M.S. and Ph.D. degrees in aerospace engineering from the University of Colorado. He is currently an Assistant Group Leader in the Mechanical Engineering Group at MIT Lincoln Laboratory. During his 13 years at MIT LL, he worked as a member of the Technical Staff in the Engineering and Space Systems Divisions, where he worked on a variety of programs including the HUSIR ground radio telescope and lunar, geo-synchronous and low-earth orbit satellite missions. Before joining MIT LL, Mark worked at QinetiQ North America on concepts for deployable apertures for satellites.



Alai Lopez graduated from the University of Texas at EL Paso in 2019 acquiring his Bachelors degree in Mechanical Engineering. After graduating, he began his work at MIT Lincoln Laboratory as an Assistant Staff in the Mechanical Engineering Group where he currently focuses on the development of mechanisms and deployable space structures.



Daniel Howe received a BS in Mechanical Engineering at George Mason University in 2017, and is currently an Associate Staff member in the Mechanical Engineering Group at MIT Lincoln Laboratory. Prior to joining the Laboratory, he operated satellites for Iridium Communications supporting the end of life for the legacy mission and the on-orbit deployment of Iridium NEXT. He joined

Lincoln Laboratory in 2020 as a contingent worker before joining as a Staff member in 2022, both in the Mechanical Engineering Group. His project work has focused on space systems and mechanisms design, and supporting project work through assembly, integration, and test phase activities. His current work focuses on delivering high quality prototypes on efficient timelines, primarily in the space domain.



Erik Thompson received his B.E. in Electrical Engineering from Stevens Institute of Technology in 2012, and his M.S. in Electrical Engineering from the University of Massachusetts Lowell in 2020. He is currently an Associate Staff member of the RF Technology Group at MIT Lincoln Laboratory, where he works on the development of SWaP constrained RF systems.



Alexander Morris attended the University of Alaska Fairbanks where he received B.S. (2011) and M.S. (2014) degrees in Electrical Engineering. He is currently an Associate Staff member at MIT Lincoln Laboratory in the RF Technology Group, where he works on development of phased array antennas and small HF receiver systems.



Alan J. Fenn (Life Fellow, 2019) received the BS degree from the University of Illinois at Chicago and MS and PhD degrees from The Ohio State University, all in electrical engineering. Dr. Fenn is a senior staff member in the RF Technology Group at MIT Lincoln Laboratory. He received the Life Fellow of the IEEE for his contributions to the theory and practice of adaptive phased array

antennas. He is an author of numerous journal articles, conference papers, and patents and five books in the field of antennas, electromagnetics, and adaptive phased array systems. Since joining Lincoln Laboratory in 1981, he has worked on many antenna, electromagnetics, and array solutions for communications, radar, and sensing applications. He developed focused near-field adaptive nulling and mutual coupling calibration techniques for testing the

performance of phased arrays. He has also patented and investigated the use of focused microwave adaptive phased arrays for cancer treatment. From 1978 to 1981, he was a senior engineer in the Antenna Systems Group at Martin Marietta Aerospace, Denver, Colorado. Dr. Fenn received the 2016 IEEE Aerospace Conference, M. Charles Fogg Best Paper Award, the IEEE Antennas and Propagation Society's 1990 H.A. Wheeler Applications Prize Paper Award, and the IEEE/URSI-sponsored 1994 International Symposium on Antennas (JINA) Award. He served as Technical Program Chair for the 2019 IEEE International Symposium on Phased Array Systems and Technology, and he was Technical Program Chair for the 2018 IEEE International Symposium on Antennas and Propagation.



Mary Knapp received a BS in Aerospace Engineering at MIT in 2011 and PhD in Planetary Science in 2018 and is currently a Research Scientist at MIT Haystack Observatory. Her research focus is the detection and characterization of exoplanetary magnetic fields via low frequency radio emission. She is currently a NIAC Fellow for GO-LoW, the Great Observatory for Long Wave-

lengths. Her additional research interests include the development of small spacecraft for astronomy and planetary science. She served as project scientist for the ASTERIA CubeSat since 2010 through launch and operations until end of mission and is currently the deputy PI for the AERO-VISTA twin CubeSat mission to study Earth's auroral radio emission.



Philip Erickson studied with the Space Plasma Physics group within Electrical Engineering at Cornell University where he earned both a B.S. and Ph.D. in Electrical Engineering. He has been a staff member at MIT Haystack Observatory for over 28 years. At MIT Haystack Observatory he leads the Geospace Group and is an Associate Director and Principal Research Scientist. His research

work involves remote sensing and scientific study of the near-Earth space environment, focusing on the ionosphere, plasmasphere, and magnetosphere. He helps to lead education and public outreach efforts for MIT Haystack Observatory and is an active member of HamSCI where he engages in encouraging amateur radio participation in scientific research.



Frank Lind studied at the University of Washington where he received a Bachelor of Science degree in Physics and a Bachelor of Science degree in Computer Science. He then joined the UW Geophysics Program and pursued studies leading to the Doctor of Philosophy in Geophysics. His work there focused on Passive Radar Observations of the Aurora Borealis. Currently he is a Re-

search Engineer at MIT Haystack Observatory where he develops and operates ground and space based radio science instrumentation.



Lenny Paritsky holds a BS in Mechanical Engineering and Physics from Tufts University and an MS in Aeronautics and Astronautics from the University of Washington. He is currently the Space Technology Lead at MIT Haystack Observatory, where he manages a growing space program and is a member of the AERO-VISTA team an upcoming twin-satellite mission to study radio emissions from the Earth's aurora. Previously, Mr. Paritsky has held leadership and design roles at Accion Systems, Busek, and Tethers Unlimited, where he has developed chemical rockets, electric propulsion systems, and novel 3D printing techniques.



Rebecca Masterson is a research scientist with MIT Kavli Institute at the Massachusetts Institute of Technology with over 15 years of experience in spacecraft design and development that includes structural design, control structure interactions, system engineering, program management, and integration and test. She was Instrument Manager and lead engineer for the OSIRIS-REx Student Collaboration Experiment, the REgolith X-ray Imaging Spectrometer (REXIS) and was the integration and test lead for TESS (Transiting Exoplanet Survey Satellite). Prior to MIT, she spent six years designing and certifying flight control modes for more than 20 space shuttle ISS assembly missions. Dr. Masterson's current research interests include model-based systems engineering, engineering management, uncertainty analysis as applied to engineering design, and integrated modeling. She holds B.S., M.S. and Ph.D. degrees in Mechanical Engineering, all from MIT.



Kristen Ammons earned a BS in Space Systems Engineering from Morehead State University (MSU) in 2020 and an MS in Aeronautics and Astronautics from MIT in 2022. She is currently a PhD student working in STARLab under Professor Kerri Cahoy. Her research focus is on using earth observation data to monitor energy infrastructure and its impacts on biodiversity in Central Appalachia. More broadly, she is interested in exploring how space technologies and systems thinking can be used to promote environmental justice. Kristen has additionally worked on several CubeSat projects including Lunar IceCube (MSU) and AeroVista (MIT) doing systems, safety, integration and testing.



Nicholas Belsten received the B.E. in electrical engineering from Vanderbilt University, Nashville, TN, in 2019, and the M.Sc. degree in aeronautics and astronautics from the Massachusetts Institute of Technology, Cambridge, MA, in 2022. He is currently pursuing the Ph.D. degree with the Department of Aeronautics and Astronautics, Massachusetts Institute of Technology. He works with Professor Kerri Cahoy at the Space Communications Astronomy and Telecommunications Laboratory (STAR Lab). His

research interests include small satellite technology demonstrations, high performance computing in space, exoplanet imaging, and orbital interferometry.



Ekaterina Kononov received B.S. and M.Eng. degrees in Electrical Engineering in 2012 and 2013 from the Massachusetts Institute of Technology. She is currently a graduate research fellow in the Department of Aeronautics and Astronautics at MIT and an associate technical staff member at Lincoln Laboratory. Her Ph.D. work is on space systems and computational imaging with vector sensor arrays. Prior to starting the Ph.D. program, Kononov worked on wireless communication and radar technology at Lincoln Laboratory and Maxim Integrated.



Cadence Payne received a BS in Space Science at Morehead State University in 2017, an SM in Aerospace Engineering at MIT in 2020, and is currently a PhD candidate in the Department of Aeronautics and Astronautics at MIT. Her research focus is the utility of miniaturized, CubeSat-based hyperspectral imagers for ocean color remote sensing of coastal regions. She is a GEM Fellow, a Matthew Isakowitz Fellow, and an IAF Future Space Leader. Her additional research interests include payload and mission design for the development of small spacecraft for earth observation and climate research. She served as a project systems engineer and mechanical lead for the Auxiliary Sensors Package on the AERO-VISTA twin CubeSat mission.